

## Supporting Information

### Efficient Catalytic hydrotreatment of Kraft Lignin to Alkylphenolics over Supported NiW and NiMo Catalysts in Supercritical Methanol

Anand Narani<sup>1</sup>, Ramesh Kumar Chowdari<sup>2</sup>, Catia Cannilla<sup>3</sup>, Giuseppe Bonura<sup>3</sup>,  
Francesco Frusteri<sup>3</sup>, Hero Jan Heeres<sup>\*,2</sup> and Katalin Barta<sup>\*1</sup>

<sup>1</sup>Stratingh Institute for Chemistry, University of Groningen,  
Nijenborgh 4, 9747 AG Groningen, The Netherlands

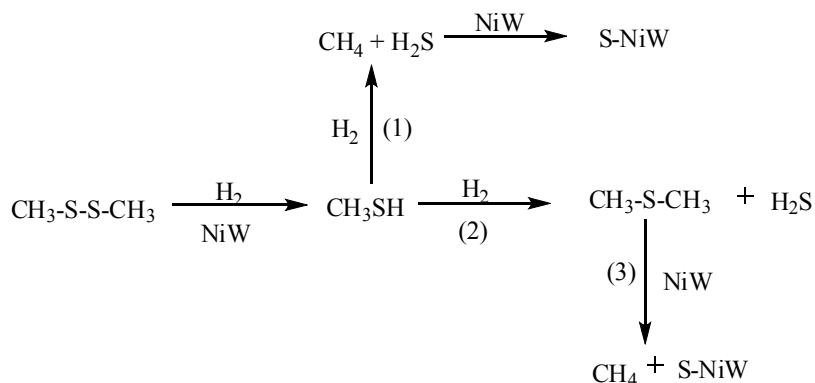
<sup>2</sup>Department of Chemical Engineering, University of Groningen,  
Nijenborgh 4, 9747 AG Groningen, The Netherlands

<sup>3</sup>CNR-ITAE, Istituto di Tecnologie Avanzate per l'Energia "Nicola Giordano",  
Via S. Lucia sopra Contesse 5, 98126 Messina, Italy

## Appendix A

### Sulphidation of the catalyst with DMDS:

Regarding the fate of the DMDS, mechanistic pathways have been proposed in the literature.<sup>1,2</sup> First, DMDS decomposes (at 280 °C) to methane thiol (CH<sub>3</sub>SH) via the hydrogenolysis of S-S bond (path 1) in the presence of H<sub>2</sub> and catalyst. Then CH<sub>3</sub>SH is further converted to methane (CH<sub>4</sub>) and H<sub>2</sub>S via path 2 and dimethyl sulphide and H<sub>2</sub>S via path 3. The formed H<sub>2</sub>S serves as sulphiding medium for formation sulphided NiW or NiMo and CoMo catalysts, by reaction of H<sub>2</sub>S with the surface metal oxides, liberating water. The formed sulphided-NiW catalyst further catalyzes dimethyl sulphide decomposition to methane and H<sub>2</sub>S in the presence of H<sub>2</sub>. The overall scheme is shown in Scheme 1.



**Scheme 1.** The fate of dimethyldisulphide during *in situ* preparation of sulphided NiMo, NiW catalysts.

The methyl groups in DMDS formed as methane ( $\text{CH}_4$ ) during the reaction which will not participate in methylation. The same excess of DMDS (0.1 g) to the reaction mixture to avoid starving of the catalyst during the reaction. We did not observe any DMDS after reaction because of its complete decomposition to  $\text{CH}_3\text{SH}$  in the presence of catalyst and  $\text{H}_2$ .

## Appendix B

### Characterization of Catalysts

*X-Ray Diffraction (XRD)* – Powdered samples were analyzed by using a *Philips X-Pert Diffractometer*, operating with a Ni  $\beta$ -filtered Cu  $K\alpha$  radiation ( $\lambda=1.5406 \text{ \AA}$ ) at 40 kV and 30 mA. Data were collected over a  $2\theta$  range of 10-100 degree, with a step size of  $0.04^\circ$  at a time per step of 3s. Diffraction peaks identification was performed on the basis of the JCPDS database of reference compounds.

*Ammonia temperature ( $\text{NH}_3$ -TPD) and carbon dioxide temperature programmed desorption ( $\text{CO}_2$ -TPD)* – Surface concentrations of acidic and basic sites were determined by temperature programmed desorption of ammonia ( $\text{NH}_3$ -TPD) and carbon dioxide ( $\text{CO}_2$ -TPD), respectively. Before TPD experiments, the catalysts (~50 mg) were reduced, at atmospheric pressure, by flowing hydrogen (60 STP ml/min) in a linear quartz micro-reactor (l, 200 mm; i.d., 4mm) from room temperature to 500 °C at a heating rate of 10 °C/min. Then, the samples were maintained under hydrogen flow at 500 °C for 30 min. After cleaning with helium, the samples were saturated for 60 min in flow of a gas mixture containing 5 vol.% of  $\text{NH}_3/\text{He}$  at 150°C or alternatively 10 vol.% of  $\text{CO}_2$  at 200 °C. In both cases the total flow rate was 25 ml/min. Then, the samples were purged in helium flow until a constant baseline level was attained. TPD measurements were performed in the temperature range 100–600 °C at a rate of 10 °C/min using helium (25 STP ml/min) as carrier flow. The evolved ammonia or carbon dioxide was detected by an on-line thermal-conductivity detector, calibrated by the peak area of known pulses of  $\text{NH}_3$  or  $\text{CO}_2$ .

*Transmission electron microscopy (TEM)* – A Philips CM12 microscope (resolution 0.2 nm), provided with a high resolution camera, at an accelerating voltage of 120 kV was used to acquire and elaborate TEM images. Suitable specimens for TEM analyses were prepared by ultrasonic dispersion in *i*-propyl alcohol adding a drop of the resulting suspension onto a holey carbon supported grid.

*Surface area ( $S_{\text{BET}}$ ), Pore Volume (PV) and Pore Size Distribution (PSD)* – Surface area, pore volume and pore size distribution were determined from the nitrogen adsorption/desorption isotherms at  $-196^\circ\text{C}$ , using a Micromeritics' ASAP2020 Instruments gas adsorption device. Before analysis, all samples were outgassed at 180°C under vacuum for 5 h. Samples containing carbon were outgassed at 180°C for 12h. The isotherms were elaborated to obtain surface area and pore volume of the investigated catalysts.

*Scanning Electron Microscopy (SEM)* – The morphology of the samples was investigated by scanning electron microscopy measurements carried out by using a *Philips XL-30-FEG Scanning Electron Microscope* at an accelerating voltage of 5-15 kV. Specimens were deposited as powders on an aluminum pin flat stubs.

*SEM-EDX and Mapping* – The qualitative and semi quantitative analysis of elemental composition has been investigated by SEM-EDX measurements, by using the Scanning Electron Microscope equipped with an Energy-Dispersive X-Ray (EDX) analyzer able to detect X-rays produced by the interaction of electrons with the sample. X-rays have also been used to form map profiles, showing the elemental distribution in the samples by using the same experimental conditions of SEM-EDX.

## Appendix C

### GC×GC-FID calibration

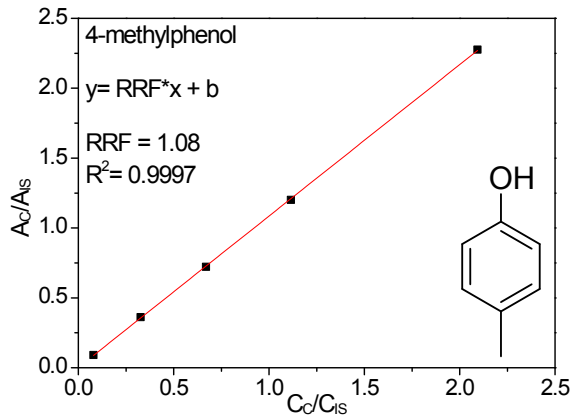
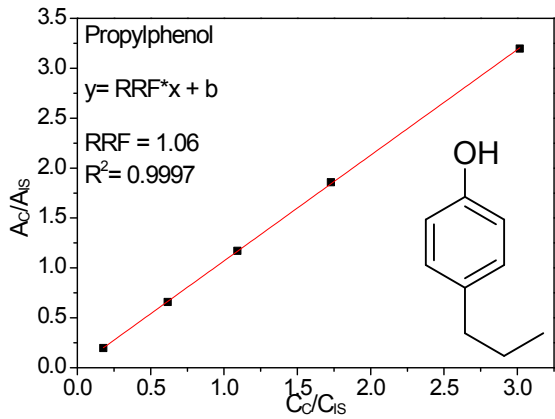
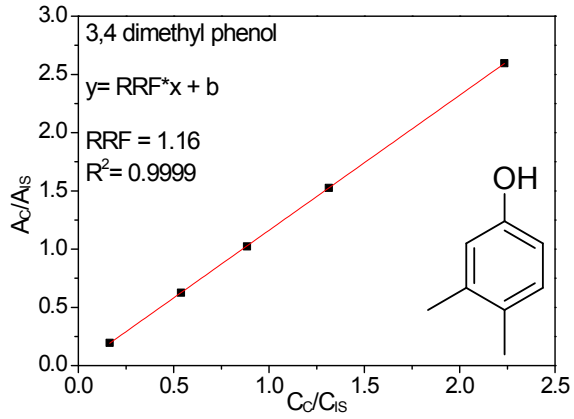
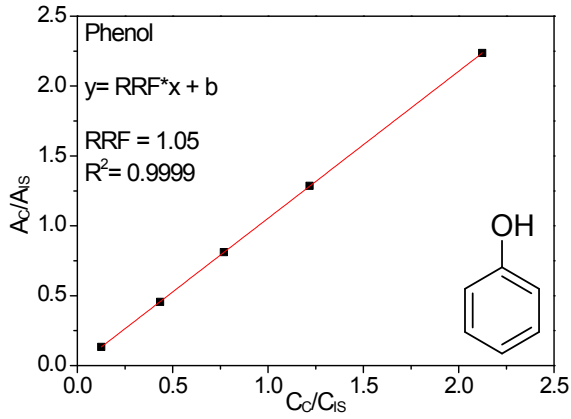
The first step in the quantification procedure involved determination of the RRF value for a number of representative model components belonging to the various compound groups (alkylphenolics, aliphatic hydrocarbons, aromatics,). The following equation was used to calculate the RRF for an individual model component:

$$RRF = \frac{C_{IS} \cdot A_c}{C_c \cdot A_{IS}}$$

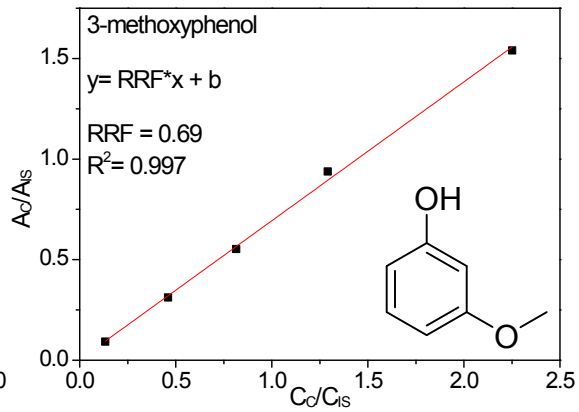
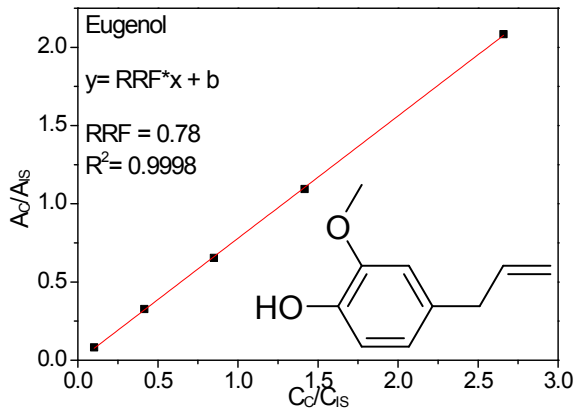
where  $C_{IS}$  is the concentration of the internal standard,  $A_{IS}$  the area of the internal standard (di-n-butylether, DBE),  $C_c$  the concentration of the component C,  $A_c$  is the area of the component, and RRF is the relative response factor for compound C.

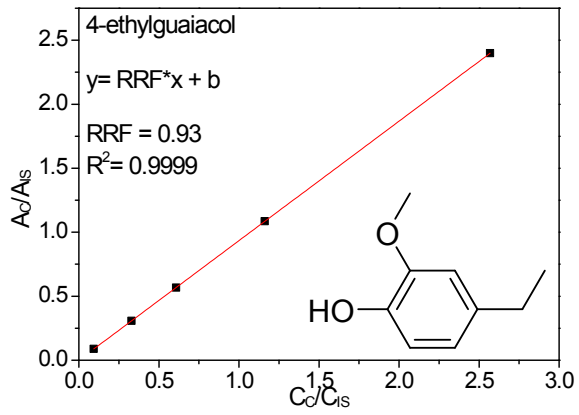
The RRF value for an individual model component was determined by plotting the ratio  $C_c/C_{IS}$  versus the ratio  $A_c/A_{IS}$ . In such a plot, (see below), the slope is the RRF value for the individual model component.

**Examples for the phenolics (alkylated) group:**

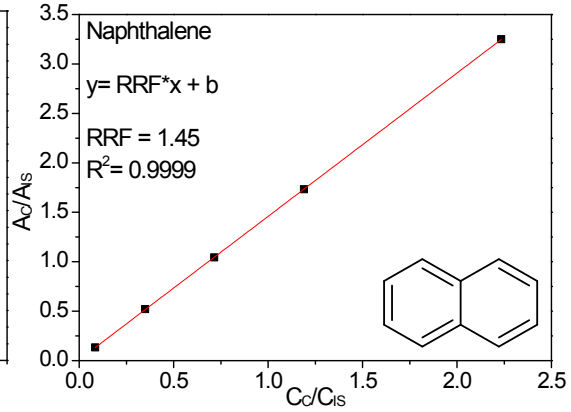
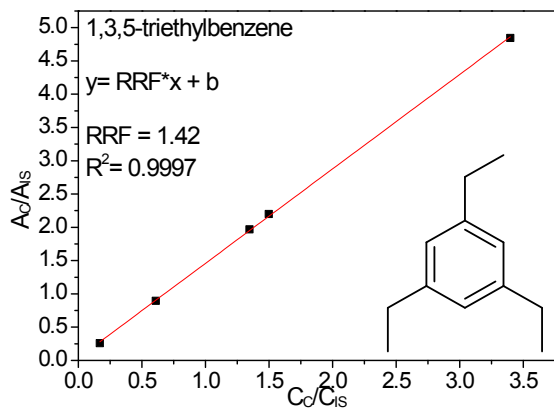
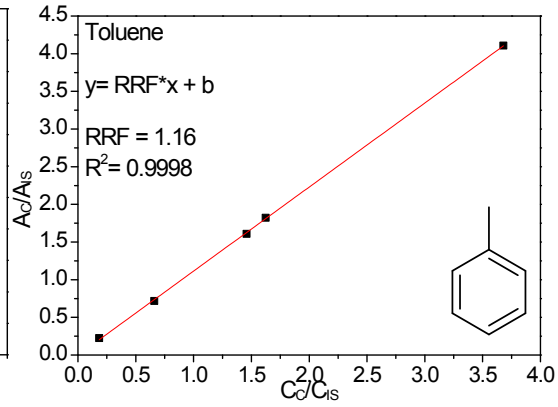
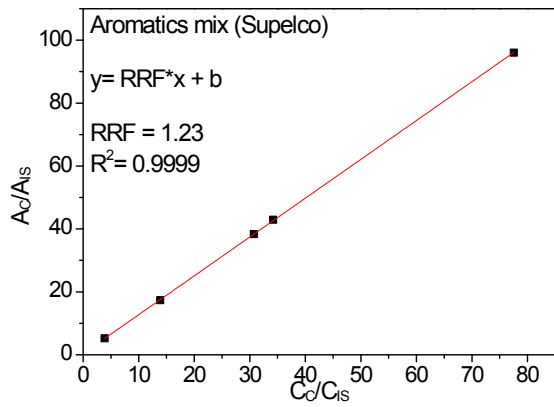


**Examples for the guaiacolics (alkylated):**





**Examples for the aromatics:**



For the quantification based on compound groups, the total compound group area was calibrated over a concentration range of 10 to 100 mg/kg by using 5 calibration mixtures. From these calibrations, an average RRF is calculated for each compound group, see Table below.

<b>Compound group</b>	<b>RRF (DBE)</b>
Alkylatedphenolics	1.1
Methoxylated alkylated phenolics	0.9
Polyaromatics/Naphthalenes	1.23
Linear/branched alkanes	1.6
Cyclic alkanes	1.5
Ketones/Alcohols	1

**Table S1** Textural properties of NiW/AC and S-NiW/AC catalysts.

<b>Entry</b>	<b>Catalyst</b>	<b>SA<sub>Lang</sub> (m<sup>2</sup>g<sup>-1</sup>)</b>	<b>PV* (cm<sup>3</sup>/g)</b>	<b>APD** (Å)</b>
1	NiW/AC	857.4	0.450	21
2	S-NiW/AC	161.2	0.158	39

\*Pore Volume determined between 5 to 600 Å (micro and mesopores)

\*\*Average Pore Diameter determined as 4PV/SA

**Table S2** Average molecular weight values determined by GPC analysis of methanol soluble oils obtained over different S-NiW catalysts

Entry	Catalyst	Average molecular weight (g/mol)
1	S-NiW/AC	500
2	S-NiW/ZSM-5	280
3	S-NiW/ML	430
4	S-NiW/MC	400
5	S-NiW/MZ	470
6	S-NiW/AC <sup>a</sup>	530
7	S-NiW/AC <sup>b</sup>	520
8	S-NiW/AC <sup>c</sup>	800
9	S-NiW/AC <sup>d</sup>	510
10	S-NiW/AC <sup>e</sup>	520
11	S-NiW/AC <sup>f</sup>	2725

Reaction conditions: catalyst (0.25 g); Kraft lignin (1 g), methanol (30 ml); H<sub>2</sub> (35 bar), time (8 h).  
<sup>a</sup>280 °C, <sup>b</sup>300 °C, <sup>c</sup>4 h, <sup>d</sup>16 h, <sup>e</sup>24 h, <sup>f</sup>DCM soluble solid

**Table S3** SEM-EDAX measurements of NiW/AC and S-NiW/AC catalysts

Sample		<i>Ni</i>		<i>W</i>		<i>C</i>		<i>O</i>		<i>S</i>		<i>Extra</i>	
		<i>wt.</i> %	<i>at.</i> %	<i>wt.</i> %	<i>at.</i> %	<i>wt.</i> %	<i>at.</i> %	<i>wt.</i> %	<i>at.</i> %	<i>wt.</i> %	<i>at.</i> %	<i>wt.</i> %	<i>at.</i> %
NiW/AC	500x	3.09	0.69	5.65	0.41	86.28	94.79	4.99	4.11				
	500x	4.40	1.06	10.88	0.83	80.19	94.13	4.52	3.98				
	1000x	4.29	1.02	10.18	0.77	81.15	94.38	4.38	3.82				
	2000x	4.25	1.02	11.17	0.86	80.69	94.70	3.89	3.43				
S-NiW/AC	500x	2.50	0.56	4.14	0.30	86.07	94.20	4.81	3.95	1.97	0.81	0.3	0.1

**Table S4** GC×GC-FID results of product distribution and total monomer yields (wt% on lignin intake) over different catalysts.

Entry	Catalyst	Alkyl phenolics (wt%)	Catechols (wt%)	Guaiacolics (wt%)	Other aromatics (wt%)	Napthalenes (wt%)	alkanes (wt%)	Total monomers (wt%)
1	NiMo/AC <sup>a</sup>	5.0	0.1	1.0	0.2	0.2	0.0	6.5
2	NiMo/AC	8.0	2.0	2.5	0.5	1.0	0.5	14.5
3	CoMo/AC	5.5	0.2	2.5	0.1	0.5	0.2	9.0
4	NiWO <sub>x</sub> /AC	6.5	1.7	7.0	0.4	0.8	0.1	16.5
5	S-WO <sub>x</sub> /AC	10.0	2.6	4.5	1.1	1.4	0.9	20.5
6	S-Ni/AC	10.5	1.0	5.5	0.9	0.6	0.5	19.0
7	S-NiW/AC	16.0	4.3	5.5	1.0	1.0	0.7	28.5
8	S-NiW/ZSM-5	11.0	0.7	4.5	1.0	0.7	0.1	18.0
9	S-NiW/ML	13.5	4.3	7.0	0.4	1.2	0.1	26.5
10	S-NiW/MC	12.0	2.9	5.0	1.0	0.9	0.7	22.5
11	S-NiW/MZ	6.0	1.7	5.5	2.1	0.8	0.4	16.5

Reaction conditions: catalyst (0.25 g); Kraft lignin (1 g); methanol (30 ml); H<sub>2</sub> (35 bar); temperature (320 °C); time (8 h).

<sup>a</sup>without external hydrogen (hydrogen free)

**Table S5** GC×GC-FID results of product distribution and total monomer yields (wt% on lignin intake) obtained over different catalysts S-NiW/AC catalyst at different temperatures.

Entry	Temperature (°C)	Alkyl phenolics (wt%)	Catechols (wt%)	Guaiacolics (wt%)	Other aromatics (wt%)	Napthalenes (wt%)	Alkanes (wt%)	Total monomers (wt%)
1	280	10.5	2.1	5.0	1.0	0.8	0.6	20.0
2	300	12.0	1.3	7.0	1.2	1.1	0.4	23.0
3	320	16.0	4.3	5.5	1.0	0.7	1.0	28.5

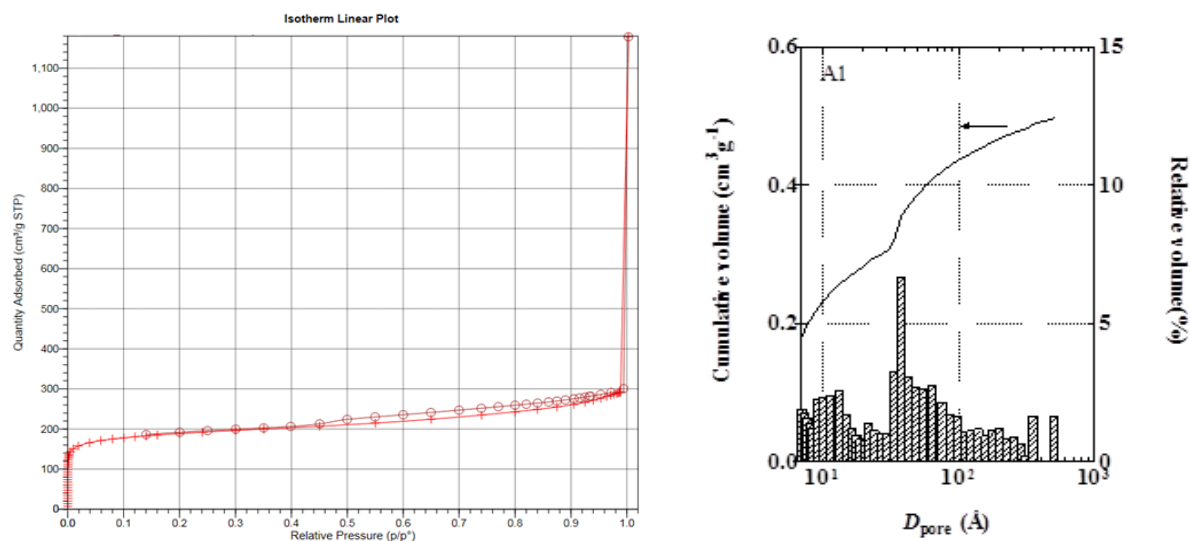
Reaction conditions: catalyst (0.25 g); Kraft lignin (1 g), methanol (30 ml); H<sub>2</sub> (35 bar), time (8 h).



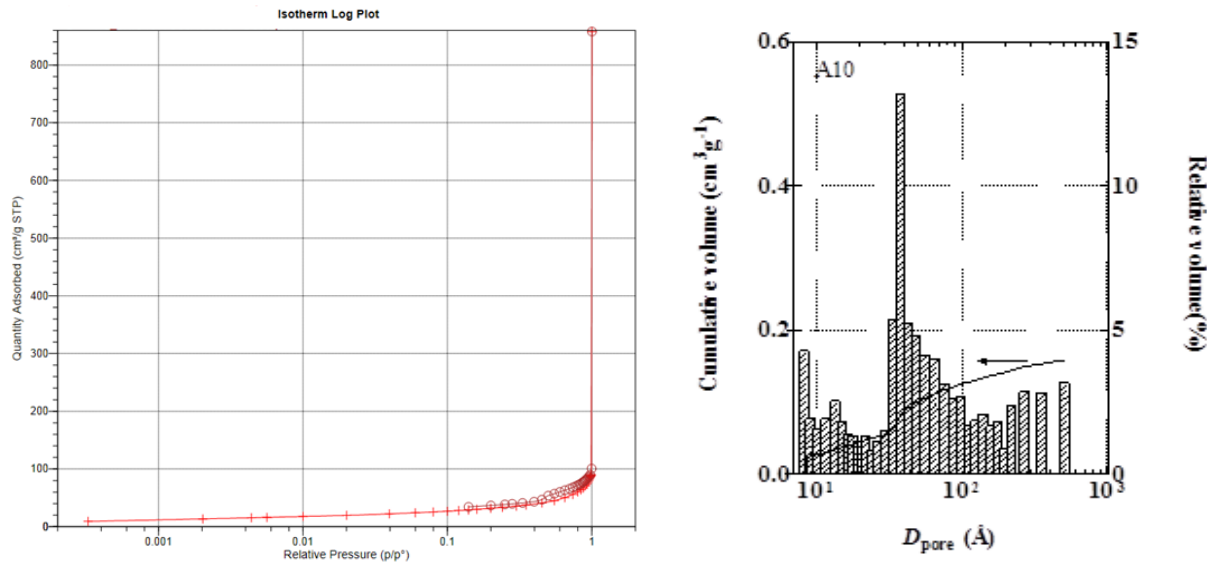
**Table S6.** Gas products obtained after reaction at 320°C in methanol for 8 h with different catalysts

Entry	Catalyst	CO <sub>2</sub> (g)	C <sub>2</sub> H <sub>4</sub> (g)	C <sub>2</sub> H <sub>6</sub> (g)	C <sub>3</sub> H <sub>6</sub> (g)	C <sub>3</sub> H <sub>8</sub> (g)	CH <sub>4</sub> (g)	CO (g)	Total (g)
1	Blank	0.6745	0.0000	0.0000	0.0000	0.0000	1.5040	0.0507	2.2300
2	NiMo/AC <sup>a</sup>	0.0205	0.0003	0.0011	0.0005	0.0000	0.0092	0.0023	0.0341
3	NiMo/AC	0.1063	0.0000	0.0007	0.0011	0.0104	0.4408	0.0067	0.5664
4	CoMo/AC	0.0321	0.0000	0.0002	0.0000	0.0029	0.0846	0.0025	0.1226
5	NiWO <sub>x</sub> /AC	0.1113	0.0001	0.0014	0.0250	0.0000	0.3283	0.0116	0.4780
6	S-WO <sub>x</sub> /AC	0.5249	0.0010	0.0057	0.1165	0.0026	1.3782	0.0409	2.0701
7	S-Ni/AC	0.1521	0.0002	0.0014	0.0352	0.0000	0.4001	0.1808	0.7701
8	S-NiW/AC	0.0384	0.0054	0.0159	0.0071	0.0000	0.2218	0.0000	0.2888
9	S-NiW/ZSM-5	0.0046	0.0060	0.0163	0.0056	0.0000	0.1533	0.0000	0.1860
10	S-NiW/ML	0.0389	0.0000	0.0004	0.0022	0.0000	0.2367	0.0052	0.2836
11	S-NiW/MC	0.3992	0.0072	0.0217	0.0104	0.0000	0.1791	0.0464	0.6644
12	S-NiW/MZ	0.0476	0.0008	0.0004	0.0000	0.0000	0.2221	0.0074	0.2777
13	S-NiW/AC <sup>b</sup>	0.1011	0.0003	0.0032	0.0003	0.0008	0.6537	0.0008	0.7678
14	S-NiW/ML <sup>b</sup>	0.1263	0.0004	0.0037	0.0004	0.0011	0.5858	0.0148	0.7329

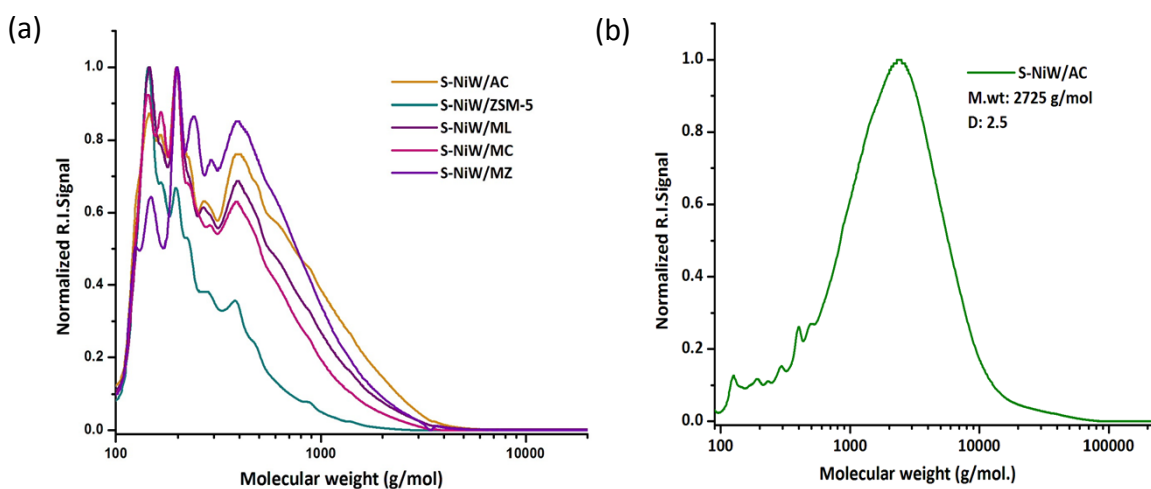
Reaction conditions: catalyst (0.25 g), Kraft lignin (1 g), methanol (30 ml), H<sub>2</sub> (3.5 MPa), temperature (320 °C), 8 h  
<sup>a</sup>without external hydrogen (Hydrogen free), <sup>b</sup>with 2g of Karft lignin



**Fig. S1** Isotherm Log Plot and Pore Size Distribution of the NiW/AC catalyst.



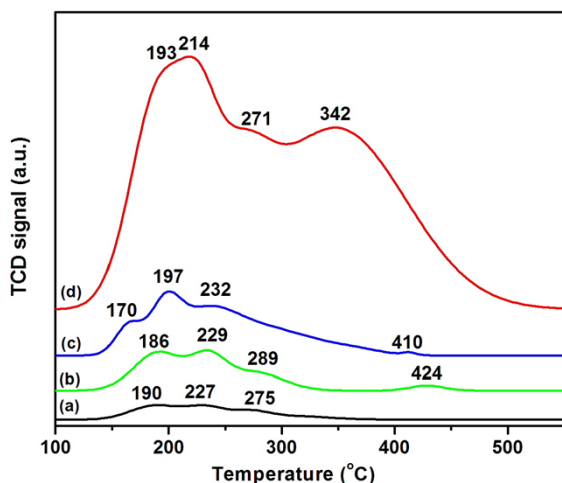
**Fig. S2** Isotherm Log Plot and Pore Size Distribution of the S-NiW/AC catalyst.



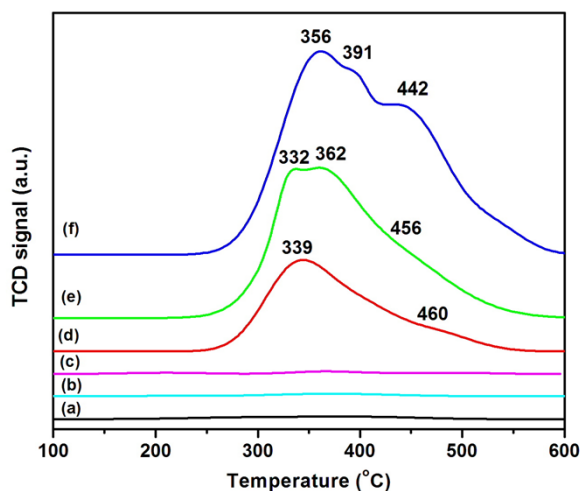
**Fig. S3** GPC molecular weight distribution of (a) methanol soluble oil fractions over NiW catalysts, (b) DCM soluble fraction over NiW/AC catalyst obtained at 320 °C for 8 h with 35 bar H<sub>2</sub>. AC (activated carbon), ML (MgO-La<sub>2</sub>O<sub>3</sub>), MC (MgO-CeO<sub>2</sub>), MZ (MgO-ZrO<sub>2</sub>)

Figure S3 shows the GPC analysis of methanol soluble oils and DCM soluble solids obtained at 320 °C for 8 h with sulphided NiW catalysts. The support plays a crucial role in catalytic hydrotreatment. With activated carbon, the average molecular weight was decreased to 500 g/mol (Figure S3-a) and, with the

basic supports, the average molecular weight further decreased to 430-470 g/mol (ML=430 g/mol, MC=400 g/mol, MZ=470 g/mol), but lower yields of methanol soluble oils (Table 1, entries 10, 11, 12) and monomers (16.5 to 26.5 wt%, Fig. 4) were obtained. In the case of acidic ZSM-5 support the average molecular weight was further lowered to 280 g/mol, but 30 wt% of char (Table 1, entry 9) was also observed. From GPC it was possible to conclude that sulphided NiW with AC support significantly depolymerise Kraft lignin (avg. Mwt. ~4000 g/mol) to low molecular weight compounds (avg. Mwt. 500 g/mol). The DCM soluble product (solid) has high molecular weight around 2725 g/mol (Figure S3-b).



**Fig. S4** NH<sub>3</sub>-TPD profiles of NiMo and NiW catalysts: (a) NiW/AC; (b) NiMo/AC; (c) CoMo/AC; (d) NiW/ZSM-5.



**Fig. S5** CO<sub>2</sub>-TPD profiles of NiMo and NiW catalysts (a) NiW/AC (b) NiMo/AC (c) CoMo/AC (d) NiW/MgO-ZrO<sub>2</sub> (e) NiW/MgO-CeO<sub>2</sub> (f) NiW/MgO-La<sub>2</sub>O<sub>3</sub>.

As it is possible to observe, all the samples show desorption patterns tightly dependent on the surface properties of the support. The ZSM5-supported NiW catalyst (Figure S4-d) shows TPD profiles fundamentally associated to ammonia desorbed from acid sites of the zeolite. So, on such catalyst the ammonia evolved between 150 and 300 °C is attributable to the desorption from weak acid sites, while the desorption peak, in the temperature region between 300 and 400 °C, is generally associated to the ammonia desorbed from stronger acid sites of the zeolite. Moreover, a minor NH<sub>3</sub> desorption is evident both on at higher temperature (400-500 °C), as the result of the presence of other sites, inducing a strong-type acidity. Instead, the total acidity measured for the NiW (Figure S4-a), NiMo (Figure S4-b) and CoMo (Figure S4-c) on carbon-supported systems was quite low, ranging from 18.4 to 77.0 μmol/g<sub>cat</sub>. Anyhow, the increase in acidity by exchanging WO<sub>x</sub> with MoO<sub>x</sub> on the carbon-supported samples (see Figure S4-a and S4-b) could be related to the textural properties of the support, allowing the presence of isolated tungstate groups on activated carbon instead allowing the formation of polymolybdate clusters, which can delocalize protons among neighboring MoO<sub>x</sub> species, so increasing the total acidity.

Summarizing, it was found that the supports plays a fundamental role in determining the total acidity. Furthermore, the substitution of NiO with CoO promotes a larger acidity too.

As shown in Figure S5, the NiW, NiMo and CoMo samples supported on activated carbon (Figure S5-a, S5-b, S5-c) exhibit a poor affinity for CO<sub>2</sub> in the investigated range of temperature. In fact, only a just drifted baseline is observable on such samples, without any appreciable difference as a consequence of the different oxide composition. The other supported catalysts, instead, exhibit a quite larger desorption band, spanned in the temperature region 250-550 °C, more or less asymmetrical and resulting as the convolution of two or three desorption maxima at least. In particular, with 104.7 μmol/g<sub>cat</sub> of CO<sub>2</sub> desorbed, the sample supported on MgO-ZrO<sub>2</sub> (Figure S5-d) displays the lowest basicity, whereas by exchanging ZrO<sub>2</sub> of the support into CeO<sub>2</sub> (Figure S5-e) or into La<sub>2</sub>O<sub>3</sub> (Figure S5-f), the basic capacity significantly increases, with CO<sub>2</sub> uptake values of 188.3 and 291.0 μmol/g<sub>cat</sub> respectively.

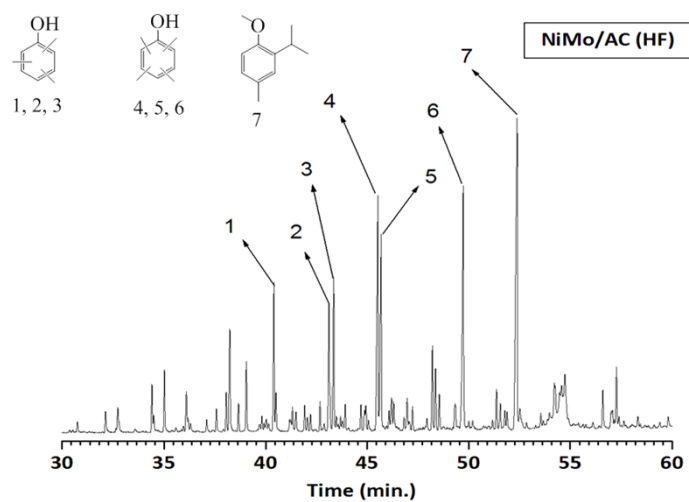


**Fig. S6** GC-MS-FID chromatogram of methanol soluble oil fraction obtained at 320 °C using S-NiMo/AC under hydrogen free for 8h.

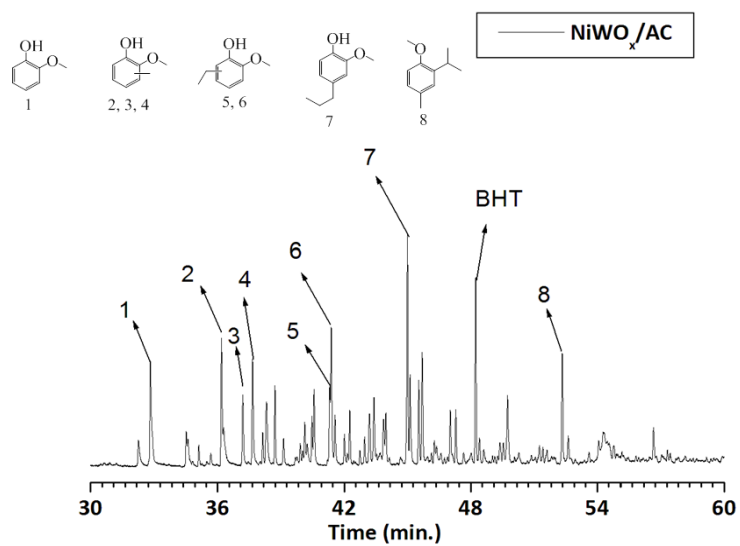


**Fig. S7** GC-MS-FID chromatogram of methanol soluble oil fraction obtained at 320 °C using non-sulphided NiWO<sub>x</sub>/AC with 35 bar H<sub>2</sub> for 8 h.

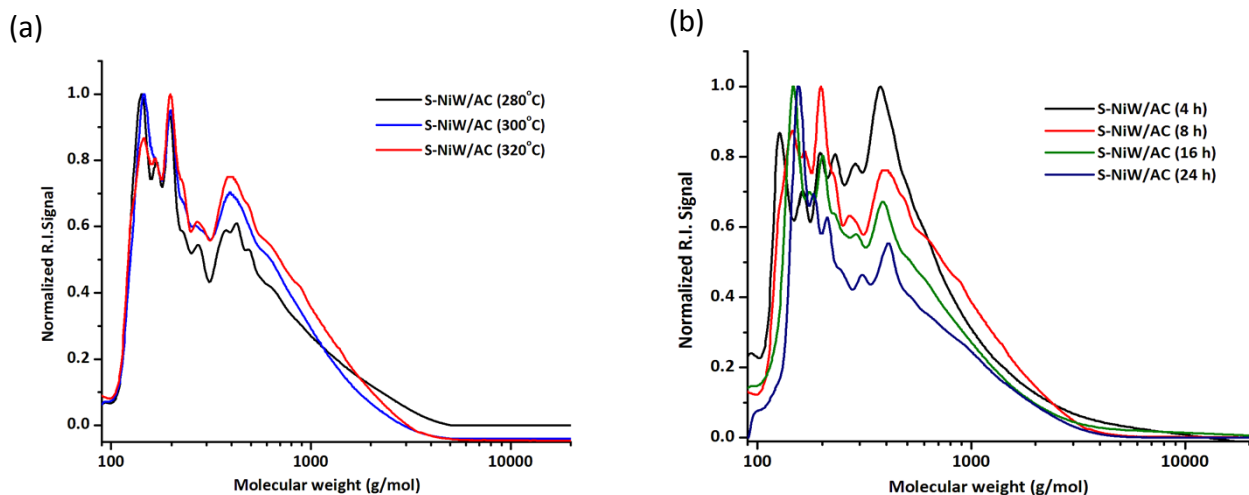


**Fig. S8** GPC molecular weight distribution of methanol soluble oil fractions over NiW/AC catalyst: (a) Effect of Temperature; (b) Effect of time.

Figure S8-a shows GPC analysis of methanol soluble oils obtained at different temperatures. More extensive depolymerization was observed with increasing temperature. The average molecular weight at 280 °C was 530 g/mol was decreased to 520 g/mol at 300°C, which was further decreased to 500 g/mol under optimum reaction temperature (320 °C). Figure S8-b explains effect of time on molecular weight distribution of methanol soluble fractions obtained at 320 °C, which reveals that the average molecular weight was 800 g/mol after 4 h of reaction time which was decreased to 500 g/mol after 8 h. As the time increasing from 8 h to 24 h there was nothing much change in molecular weight distribution.

## Appendix D

Formulas used for calculation of monomer yields (wt%), methanol soluble oil (wt%), DCM, DMSO soluble solids and yields of char (wt%):

$$\text{Monomers yields (wt\%)} = \frac{\text{weight of monomers (calculated from 2D GC)}}{\text{Initial kraft lignin wt.}} \times 100$$

$$\text{Methanol soluble oil (wt\%)} = \frac{\text{Methanol soluble oil wt.}}{\text{Initial kraft lignin wt.}} \times 100$$

$$\text{DCM soluble products (wt\%)} = \frac{\text{DCM soluble products wt.}}{\text{Initial kraft lignin wt.}} \times 100$$

$$\text{DMSO soluble solids (wt\%)} = \frac{\text{DMSO soluble solid wt.}}{\text{Initial kraft lignin wt.}} \times 100$$

$$\text{Yield of Char (wt\%)} = \frac{\text{Insoluble solid wt.}}{\text{Initial kraft lignin wt.}} \times 100$$

### References:

[1] L. Ding and Y. Zheng, *Catal. Commun.*, 2006, **7**, 1035.

[2] F. Bataille, J.L. Lemberon, G. Pérot, P. Leyrit, T. Cseri, N. Marchal and S. Kasztelan, *Appl. Catal. A*, 2001, **220**, 191.